Stochastic dynamics on slow manifolds

George W A Constable[1], Alan J McKane[1], Tim Rogers[2]

[1] Theoretical Physics, School of Physics and Astronomy, The University of Manchester, Manchester M13 9PL, UK

[2] Department of Mathematical Sciences, University of Bath, Claverton Down, Bath BA2 7AY, UK

Abstract. The theory of slow manifolds is an important tool in the study of deterministic dynamical systems, giving a practical method by which to reduce the number of relevant degrees of freedom in a model, thereby often resulting in a considerable simplification. In this article we demonstrate how the same basic methodology may also be applied to stochastic dynamical systems, by examining the behaviour of trajectories conditioned on the event that they no not depart the slow manifold. We apply the method to a pair of example models from ecology and epidemiology, achieving a reduction in model dimension and gaining excellent analytical approximations.

PACS numbers:

1. Introduction

It is possibly only a slight exaggeration to say that of all the mathematical models we can dream of, there are only two kinds which are straightforward to solve: those which are linear, and those which are one-dimensional. This aphorism holds equally for stochastic dynamical systems as it does for their deterministic counterparts. Much of applied mathematics and theoretical physics is devoted to the delicate art of taking high-dimensional or non-linear problems of interest and finding appropriate approximation schema by which to reduce their apparent difficultly.

The theory of slow manifolds is an example just such a scheme and one which is well developed for deterministic dynamical systems [9]. In many models of interest there exists a separation of time scales between some quantities which relax very quickly to an essentially static value, and others which change more slowly and can be sensitive to perturbations. The term 'slow manifold' describes the space in which these slower quantities vary, after the fast initial transient has died out. Restricting attention to this space offers an effective method by which to remove the so-called fast degrees of freedom from the model, thereby reducing the dimension and simplifying the system. Our goal in this article is to show that the ideas of slow manifold theory from deterministic systems may be put to good use in stochastic systems as a tool to remove fast degrees of freedom.

The removal of fast variables from stochastic systems has generated a significant amount of attention and has led to a variety of approximation methods. The biggest difference between these methods is the framework within which the stochastic system is represented; stochastic differential equations, which are similar to ordinary differential equations with a stochastic noise term, or the master equation representation, a partial differential equation describing the evolution of the probability distribution of states. Among existing techniques the Haken slaving principle [10] [7] [8] and the projector method developed by Gardiner [3] are perhaps the most ubiquitous. It is useful therefore to briefly describe these methods, along with a 'naive' procedure, direct adiabatic elimination, in order to clarify the differences between them and the method developed here.

The direct adiabatic elimination method is one which is formulated to act on a set of stochastic differential equations (SDE's) describing some system. The procedure mirrors closely that of slow manifold theory: the variables associated with the fast dynamics are assumed to be stationary, from which a function describing the slow manifold may be determined. In the naive stochastic analogue, the function determining the manifold contains a stochastic variable. In this way the slow manifold is allowed to fluctuate. This method is often used successfully in systems where noise only acts on a limited number of the noise terms REF BROWNIAN PARTICLE and in which the entire system is linear in the fast variable. However, if non-linearities of the fast-variable exist, the elimination procedure results in mathematically ill defined noise terms [14].

The Haken slaving principle also considers a form of slow manifold approximation in an SDE framework. Yet again, the manifold itself is assumed to be vary as a function

of the noise in the fast direction. While it is derived in a far more mathematically rigorous way than the naive elimination method, it too concerns itself with uncorrelated noise terms and suffers from some of the same problems as the naive method. Namely, the approximation can yield equations for the behaviour on the slow manifold that contain ill defined noise components. In addition, the approximated system can have a non-markovian character which leads to further complications in the analysis.

The projector method, in contrast to the naive method and the Haken slaving principle, conducts fast variable elimination in the stochastic setting of the master equation. It is perhaps the most mathematically rigorous of the methods here discussed not least because it avoids the ambiguities associated with stochastic calculus. The heart of the method is using a constructed projector operator to integrate out the dependence of the master equation on the fast variables. This results in an exact generalised non-markovian master equation for the remaining slow variables. It is to this that a fast variable elimination procedure is used, in the form of perturbative expansions and approximations on the nature of the resultant memory kernel. Whilst rigorous, the projector method is mathematically cumbersome and becomes even more so if one needs to change the variables of the initial master equation in order to separate the fast and slow directions. -

The core of our approach is to examine the behaviour of the stochastic system in the an SDE framework under the condition that its trajectories are *confined* to the slow manifold. If the noise terms in the SDE's considered are linearly independent, this amounts to simply ignoring the noise in the fast direction. A static description of the slow manifold is then at hand, devoid of fluctuating terms, allowing application to a broad ed range of slow manifold function forms than the direct elimination procedure or the Haken slaving principle. As we will see, if the noise terms are linearly dependent, the approximation differs from that obtained by simply projecting onto the slow manifold because enforcing the constraint changes the correlation structure of the stochastic fluctuations. In addition one gains a sense of physical intuition as to the behaviour of the system, which is arguably not present in the master equation setting.

The SDE's used here are developed as a limiting form of a master equation. This representation is frequently used in problems where the noise is intrinsic to the system, such as demographic noise. In such systems, it is often highly unlikely that the derived noise terms are linearly independent, and as such cross-correlations must be considered.

The use of this slow manifold approximation will also be considered in conjunction with other stochastic approximation techniques. The linear noise approximation (LNA, or Van Kampen expansion [15]) has recently found favour amongst theoreticians studying the behaviour of stochastic systems composed of many interacting agents [**?**]. In the limit of large system size, the LNA provides a macroscopic description of the system in terms of a linear stochastic differential equation (SDE). Being linear, this equation is, of course, solvable. The price paid for this simplification is that the theory only applies in the neighbourhood of an attractive fixed point of the noise-free version of the model.

In the context of the LNA, slow manifolds can be a malign presence. If some eigenvalues of the approximate linear SDE are close to zero, then a small stochastic fluctuation in the direction of the corresponding eigenvector can carry the system very far from the steady state into regions in which the true non-linear nature of the model is important. Moreover, a large separation between eigenvalues can in some situations lead to the numerical evaluation of theoretical solutions becoming ill-conditioned. Both of these effects can lead to a very poor agreement between stochastic simulations and the LNA theory.

In the next section we develop the method with the aid of a simple motivating example from ecology, before providing a general formulation. The result from this example model show how the approximation is successful even in a regime where the fixed point is weakly unstable; this addresses the first difficulty with slow manifolds and the LNA identified above. In section three we go on to apply the general formulation of the method to an epidemiological model with seasonal forcing. This model has identified as suffering from the technical numerical difficulties associated with a large separation between eigenvalues [13]. We show how our method may be used in tandem with the LNA to provide a very good approximation to results coming from stochastic simulations.

2. Method

2.1. Motivation

We begin by recapping the very basics of slow manifolds in deterministic systems. Consider the ordinary differential equation

$$\frac{d\boldsymbol{x}}{dt} = \boldsymbol{A}(\boldsymbol{x})\,, \tag{1}$$

where $\boldsymbol{x}$ is an n-dimensional vector describing the state of the system, and $\boldsymbol{A}$ is an n-dimensional vector-valued function of $\boldsymbol{x}$. As is well known, the behaviour of the system in the neighbourhood of a fixed point $\boldsymbol{x}_*$ is described by the linearisation of $\boldsymbol{A}$ around that point. Define the Jacobian matrix J with entries

$$J_{ij} = \frac{\partial}{\partial x_j} A_i(\boldsymbol{x})\Big|_{\boldsymbol{x}=\boldsymbol{x}_*}\,. \tag{2}$$

Then for $\boldsymbol{x}$ close to $\boldsymbol{x}_*$, the time evolution of the error $\boldsymbol{\xi} = \boldsymbol{x} - \boldsymbol{x}_*$ obeys

$$\frac{d\boldsymbol{\xi}}{dt} = J\boldsymbol{\xi}\,. \tag{3}$$

Further insight is gained by considering the eigenvalues and eigenvectors of J. From (3), we learn that if $\boldsymbol{v}$ is a left eigenvector of J with eigenvalue λ, then errors in the direction of $\boldsymbol{v}$ will grow exponentially if $\lambda > 0$ and shrink exponentially if $\lambda < 0$. If, on the other hand, $\lambda = 0$ then we do not know what effect perturbations in the direction of $\boldsymbol{v}$ will have on the long-term behaviour of the system. To answer this question would require a more detailed non-linear analysis, which is likely to be very difficult in a general system with several degrees of freedom. Slow manifold theory offers a way to make progress in this case by reducing the dimension of the model.

The basic observation behind the theory is as follows: since perturbations in the direction of stable/unstable eigenvectors will shrink/grow exponentially, the only trajectories whose behaviour is in question are those which are tangential to the span of the eigenvectors with eigenvalue 0. Very often, this set of eigenvectors has many fewer members than there are degrees of freedom in the original system, and thus restricting attention to this subspace achieves a considerable reduction in dimensionality.

Slow manifolds are also of great practical use when no eigenvalues are precisely zero, but there is a separation of time-scales. For example, suppose a stable fixed point $\boldsymbol{x}_*$ has associated eigenvalues satisfying $\mathrm{Re}[\lambda_1] < \ldots < \mathrm{Re}[\lambda_m] \ll \mathrm{Re}[\lambda_{m+1}] < \ldots < 0$. Perturbations in the direction of eigenvectors $\boldsymbol{v}_1\,, \ldots\,, \boldsymbol{v}_m$ will decay extremely rapidly in comparison with those in the directions of $\boldsymbol{v}_{m+1}\,, \ldots\,, \boldsymbol{v}_n$. For practical purposes, the 'slow' manifold of trajectories tangent to these less stable eigenvectors defines an $(n-m)$-dimensional system which will provide a good qualitative approximation to the behaviour of the larger system, as perturbations away from this manifold will very quickly collapse.

The goal of this article is to apply the basic ideas of slow manifolds to stochastic systems, as a tool to eliminate fast degrees of freedom. Our starting point will be

the stochastic differential equation (SDE) derived from a microscopic description of an individual based model

$$\frac{d\boldsymbol{x}}{dt} = \boldsymbol{A}(\boldsymbol{x}) + \boldsymbol{\eta}(t)\,, \tag{4}$$

where $\boldsymbol{x}$ and $\boldsymbol{A}$ are as in (1), and $\boldsymbol{\eta}$ is a vector if Gaussian white-noise variables with correlations

$$\Big\langle \eta_i(t)\eta_j(t') \Big\rangle = \varepsilon\,\delta(t-t')B_{ij}(\boldsymbol{x})\,. \tag{5}$$

Here $\langle\cdots\rangle$ denotes averaging over the noise, ε is a small parameter governing the strength of the noise, B is a matrix-valued function of the system state, and the SDE (4) is to be interpreted in the Itō sense. The details of moving from the microscopic, individual model to the macroscopic diffusion limit which the SDE describes, are outlined for the reader in Appendix A.

We are interested in the case that the deterministic ($\varepsilon = 0$) system exhibits a slow manifold. How will the stochastic system behave if we confine its trajectories to this slow manifold? We develop the theory with the aid of a specific example.

2.2. Illustrative example

To illustrate our method, we explore the behaviour of a simplistic ecological model of two interacting populations, labelled X and Y. Individuals of both populations reproduce with rate one, and there is a small probability μ of the offspring mutating from one type to the other. The organisms also prey on each other with rate ε and a slight preference p for prey of the opposite type. The model may be written in the traditional notation of chemical reaction systems:

$$\begin{aligned}
&\text{Reproduction:} && X \xrightarrow{1-\mu} X+X\,, \quad Y \xrightarrow{1-\mu} Y+Y \\
&\text{Mutation:} && X \xrightarrow{\mu} X+Y\,, \quad Y \xrightarrow{\mu} X+Y \\
&\text{Predation:} && X+Y \xrightarrow{\varepsilon(1/2+p)} X\,, \quad X+Y \xrightarrow{\varepsilon(1/2+p)} Y \\
&\text{Cannibalism:} && X+X \xrightarrow{\varepsilon(1/2-p)} X\,, \quad Y+Y \xrightarrow{\varepsilon(1/2-p)} Y\,.
\end{aligned}$$

Here arrows denote possible reactions and the values above the rate constants. Writing n_X and n_Y for the number of individuals in each population, the model may be mathematically formulated as a master equation describing the time evolution of the probability distribution $P(n_X, n_Y)$. Stochastic simulations of the model can be performed efficiently using the Gillespie algorithm [**?**].

When the predation rate ε is small, the population may grow very large. Performing an expansion of the master equation in the limit of small ε yields an effective description of the system in terms of an SDE for the scaled variables $x = \varepsilon n_X$ and $y = \varepsilon n_Y$. Details of how to perform this expansion in the general case can be found in [**?**]. For the present model, we find the following pair of equations:

$$\begin{aligned} \frac{dx}{dt} &= x - \mu(x-y) - x\left(\frac{1}{2}(x+y) - p(x-y)\right) + \eta_x(t)\,, \\ \frac{dy}{dt} &= y + \mu(x-y) - y\left(\frac{1}{2}(x+y) + p(x-y)\right) + \eta_y(t)\,, \end{aligned} \tag{6}$$

where η_x and η_y have the correlation structure specified in (5), with

$$B = \begin{pmatrix} x + \frac{1}{2}x(x+y) - (px+\mu)(x-y) & 0 \\ 0 & y + \frac{1}{2}y(x+y) + (py+\mu)(x-y) \end{pmatrix}. \tag{7}$$

We begin by examining the deterministic system found by putting $\varepsilon = 0$. There is a trivial fixed point at $x^* = 0\,,\, y^* = 0$, representing the extinct state, which is always unstable. There is second fixed point at $x^* = 1\,,\, y^* = 1$, representing equal coexistence of the two populations, this state is stable when $p < \mu$. If p is raised above μ, a supercritical pitchfork bifurcation occurs, with the equal coexistence fixed point becoming unstable and giving rise to a symmetric pair of stable fixed points in which one species dominates the other. The new fixed points have coordinates

$$x^* = \frac{1 - 2\mu \pm \sqrt{(1-\mu/p)(1-2\mu)}}{1-2p}\,,\; y^* = \frac{1 - 2\mu \mp \sqrt{(1-\mu/p)(1-2\mu)}}{1-2p}\,. \tag{8}$$

We are interested in examining the effect of noise near this transition.

The eigenvalues of the Jacobian at the coexistence state are -1 and $2(p-\mu) = \lambda$, with corresponding eigenvectors $(1,1)$ and $(1,-1)$. If $|\lambda| \ll 1$ then we have a slow manifold in the direction of $x - y$, meaning that perturbations to the balance of populations evolve very slowly. Formally, the slow manifold is defined by the collection of trajectories which are tangent to the slow eigenvector at the fixed point, although in practice there is unlikely to be a closed analytic expression for this surface. To make progress we approximate the slow manifold by the nullcline of the fast eigenvector. In the present model, the nullcline of the fast direction $x + y$ is the hyperbola

$$(x+y) - \frac{1}{2}(x+y)^2 + p(x-y)^2 = 0\,. \tag{9}$$

The two plots in figure 1 capture the typical behaviour of the model for parameters either side of the transition.

The SDE system (7) is two-dimensional, non-linear and has noise correlations which depend on the state of the system. These factors combine to make the theoretical analysis of the model very difficult. The situation is not hopeless, however, as it is clearly visible in Fig.1 that the system does not typically stray very far from one-dimensional subspace defined by the nullcline of the fast variable $x + y$. We intend to

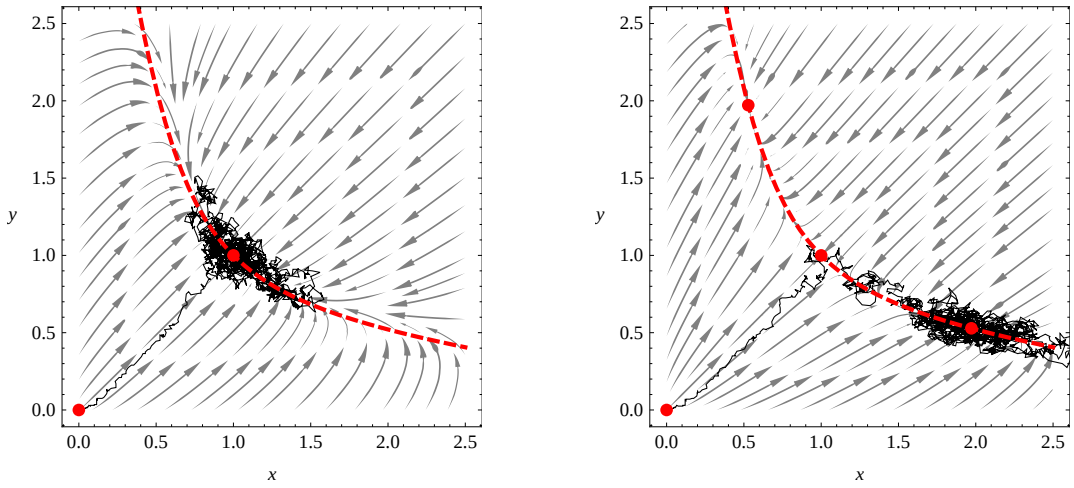

Figure 1. These plots show the behaviour of our example ecological model either side of the pitchfork bifurcation. The fixed points are shown as red circles, and the dashed red line is the nullcline $dx/dt + dy/dt = 0$, given in equation (9). The grey arrows show trajectories of the deterministic system, while the black line traces out the trajectory of a single (short) stochastic simulation of the individual-based model, starting close to the origin. The parameters are $\varepsilon = 0.005$ and $p = 0.3$ in both plots, while $\mu = 0.35$ on the left and $\mu = 0.25$ on the right.

exploit this fact to produce an 'effective' one-dimensional description of the model. The plan of attack is as follows: first we will make a coordinate transform to separate the fast and slow variables; then we will examine the behaviour of the slow variable under the assumption that the fast variable relaxes instantaneously to its nullcline value.

We introduce $w = x + y$ and $z = x - y$, so that

$$\begin{pmatrix} w \\ z \end{pmatrix} = \begin{pmatrix} 1 & 1 \\ 1 & -1 \end{pmatrix} \begin{pmatrix} x \\ y \end{pmatrix} . \tag{10}$$

In the new coordinates the nullcline is described by the equation $w - w^2/2 + pz^2 = 0$, and equation (7) becomes

$$\begin{aligned} \frac{dw}{dt} &= w - \frac{1}{2}w^2 + pz^2 + \eta_w(t) \,, \\ \frac{dz}{dt} &= z\left(1 - 2\mu - \left(\frac{1}{2} - p\right) w\right) + \eta_z(t) \,. \end{aligned} \tag{11}$$

To determine the correlation structure of the new noise variables η_w and η_z, we apply a general result about Gaussian random variables:

> Suppose that a vector of Gaussian random variables $\boldsymbol{\eta}$ has correlation matrix B, and that $\boldsymbol{\zeta} = V\boldsymbol{\eta}$ for some matrix V. Then the correlation matrix for $\boldsymbol{\zeta}$ is given by VBV^T.

In the present case, the matrices B and V are given in equations (7) and (10), respectively. We thus find the following correlation matrix for η_w and η_z:

$$B' = \begin{pmatrix} w + \frac{1}{2}w^2 - pz^2 & z(1 - 2\mu + w(\frac{1}{2} - p)) \\ z(1 - 2\mu + w(\frac{1}{2} - p)) & w + \frac{1}{2}w^2 - pz^2 \end{pmatrix} . \tag{12}$$

Notice that whilst the original noise variables η_x and η_y were independent (that off-diagonal entries of B were zero), the noise variables in the new coordinates are correlated with each other.

To enforce the assumed separation of time-scales between w and z, we impose the following conditions:

$$w = 1 + \sqrt{1 + 2pz^2}\,, \quad \text{and} \quad \eta_w(t) \equiv 0\,. \tag{13}$$

The first of these sets w to its equilibrium value for a given z (that is, the corresponding point on the nullcline), whilst the second removes the possibility of any noise-induced fluctuations. What effect do these constraints have on the evolution of z? First, we may substitute $w = 1 + \sqrt{1 + 2pz^2}$ into (12) to remove the dependence on w, thus

$$\frac{dz}{dt} = f(z) + \eta_z(t)\,, \tag{14}$$

where

$$f(z) = z\left(1 - 2\mu - \left(\frac{1}{2} - p\right)\left(1 + \sqrt{1 + 2pz^2}\right)\right) . \tag{15}$$

Second, we must determine the effect of the conditions on the noise variable η_z. Since η_w and η_z are correlated, imposing $\eta_w = 0$ will alter the statistical distribution of η_w. Again we apply a general result about correlated Gaussian random variables:

> Suppose that a collection of Gaussian random variables $(\eta_1, \ldots, \eta_n)$ has correlation matrix B. Let B' be the correlation matrix of $(\eta_2, \ldots, \eta_n)$ conditioned on the event that $\eta_1 = 0$. Then B' and B are related by
>
> $$[B'^{-1}]_{ij} = [B^{-1}]_{ij}\,, \quad \text{for all} \;\; i, j = 2, \ldots, n\,. \tag{16}$$
>
> In particular, if $n = 2$ then the variance of η_2 conditioned on $\eta_1 = 0$ is
>
> $$B' = B_{22} - \frac{B_{12}B_{21}}{B_{11}}\,. \tag{17}$$

Applying formula (17) to the correlation matrix found in (12), we obtain

$$\langle \eta_z(t)\eta_z(t') \rangle = \varepsilon\, \delta(t - t') g(z)\,. \tag{18}$$

The noise strength g is given by the slightly complicated expression

$$g(z) = \left(w + \frac{1}{2}w^2 - pz^2\right)\left(1 - \left(z\frac{1 - 2\mu + w(\frac{1}{2} - p)}{w + \frac{1}{2}w^2 - pz^2}\right)^2\right) , \tag{19}$$

where of course $w = 1 + \sqrt{1 + 2pz^2}$.

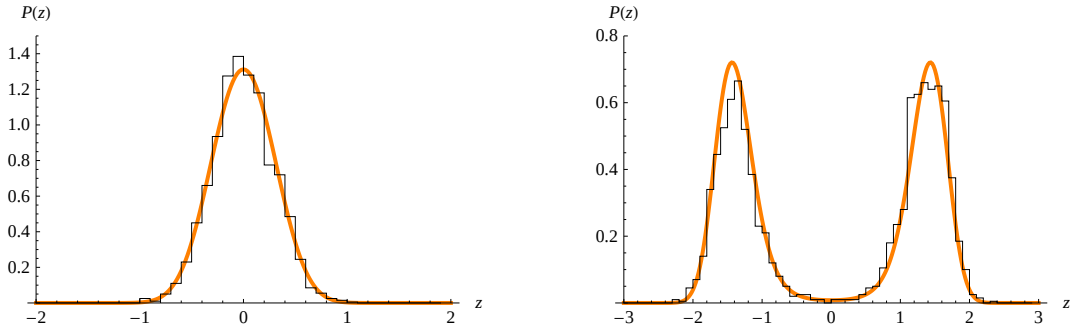

Figure 2. The stationary distribution of $z = x - y$ as predicted by the reduced-dimension model (orange curve) and measured from a single long simulation run of the individual-based model (black histogram). The parameters are the same as those in Fig. 1. The theoretical prediction was obtained by numerically integrating Eq. (20), with parameters taken from Fig. 1, whilst 2000 data points were collected from simulation run at time intervals of 100.

Equations (14) and (18) together define a one-dimensional stochastic differential equation. Although it may look like an almighty mess, since it is one-dimensional most questions of interest about this system can be answered by textbook methods [4]. For example, the long-time average behaviour of the model is captured in the stationary distribution of z, which has the following explicit form:

$$P(z) = \frac{1}{g(z)} \exp\left(\frac{2}{\varepsilon}\int_{-\infty}^{z} \frac{f(z')}{g(z')}\, dz'\right) . \tag{20}$$

In figure 2 we compare the analytical prediction of equation (20) with a histogram of the z-coordinate of the sample points of stochastic simulations taken from figure 1. Clearly, the reduced one-dimensional model provides a very good fit to the data coming from the individual-based simulation. It should also be pointed out that although we have developed the theory based on the local behaviour around the coexistence fixed point $(1, 1)$, the approximation remains successful even in the unstable regime.

2.3. General formulation

We close this section by providing a description of the method for an arbitrary n-dimensional SDE

$$\frac{d\boldsymbol{x}}{dt} = \boldsymbol{A}(\boldsymbol{x}) + \boldsymbol{\eta}(t)\,, \tag{21}$$

with noise correlations

$$\Big\langle \eta_i(t)\eta_j(t')\Big\rangle = \varepsilon\,\delta(t-t')\Big[B(\boldsymbol{x})\Big]_{ij} . \tag{22}$$

Suppose we are interested in behaviour around a fixed point $\boldsymbol{x}_*$. Let J be the Jacobian of $\boldsymbol{A}$ at that point and write $\lambda_1, \ldots, \lambda_n$ for its eigenvalues. Suppose further that λ_1 is non-degenerate, real and very negative, and thus its associated eigenvector $\boldsymbol{v}_1$ represents a very stable direction. We aim to eliminate fluctuations in this direction to produce

a reduced-dimension model. To apply our method, we first make a change of variables from the n-vector $\boldsymbol{x}$ to a single variable y and an $(n-1)$-vector $\boldsymbol{z}$, via the coordinate transformation

$$\begin{pmatrix} y \\ \boldsymbol{z} \end{pmatrix} = V\boldsymbol{x}\,. \tag{23}$$

It is always possible to choose V so that

$$J' = VJV^{-1} = \begin{pmatrix} \lambda_1 & 0 \\ 0 & L \end{pmatrix}, \tag{24}$$

where L is an $(n-1)\times(n-1)$ matrix. The first row of V must be $\boldsymbol{v}^T$, and therefore near the fixed point $\boldsymbol{x}_*$, the variable y describes the distance from the slow manifold along the fast direction $\boldsymbol{v}$, while the remaining $n-1$ slow degrees of freedom are captured by $\boldsymbol{z} = (z_2, \ldots, z_n)^T$. In the new coordinates the SDE becomes

$$\frac{d}{dt}\begin{pmatrix} y \\ \boldsymbol{z} \end{pmatrix} = V\boldsymbol{A}\left(V^{-1}\begin{pmatrix} y \\ \boldsymbol{z} \end{pmatrix}\right) + \boldsymbol{\zeta}(t)\,, \tag{25}$$

where

$$\Big\langle \zeta_i(t)\zeta_j(t')\Big\rangle = \varepsilon\,\delta(t-t')\Big[B'(y,\boldsymbol{z})\Big]_{ij}\,, \tag{26}$$

and $B' = VBV^T$. We wish to constrain y to its nullcline, which is defined by the equation

$$\boldsymbol{v}^T\boldsymbol{A}\left(V^{-1}\begin{pmatrix} y \\ \boldsymbol{z} \end{pmatrix}\right) = 0\,. \tag{27}$$

Local to the fixed point the nullcline is very well approximated by the hyperplane $y = 0$, although in general it will have a more complex form (such at the hyperbola in the ecological example). We will assume that we may unambiguously describe the nullcline by a known function $y = \theta(\boldsymbol{z})$.

To enforce the assumed separation of time-scales between y and the other variables, we impose the following conditions:

$$y = \theta(\boldsymbol{z})\,, \quad \text{and} \quad \zeta_1(t) \equiv 0\,. \tag{28}$$

For the remaining variables, we have

$$\frac{d\boldsymbol{z}}{dt} = \boldsymbol{A}''(\boldsymbol{z}) + \boldsymbol{\zeta}(t)\,, \tag{29}$$

where

$$\Big\langle \zeta_i(t)\zeta_j(t')\Big\rangle = \varepsilon\,\delta(t-t')\Big[B''(\boldsymbol{z})\Big]_{ij}\,. \tag{30}$$

The drift vector $\boldsymbol{A}''(\boldsymbol{z})$ and diffusion matrix $B''(\boldsymbol{z})$ are derived from $\boldsymbol{A}$ and B as follows. For $i, j = 2, \ldots, n$

$$\Big[\boldsymbol{A}''(\boldsymbol{z})\Big]_i = \left[V\boldsymbol{A}\left(V^{-1}\begin{pmatrix} \theta(\boldsymbol{z}) \\ \boldsymbol{z} \end{pmatrix}\right)\right]_i \tag{31}$$

and

$$\Big[B''(\boldsymbol{z})^{-1}\Big]_{i,j} = \Big[B'(\theta(\boldsymbol{z}),\boldsymbol{z})^{-1}\Big]_{ij}\,. \tag{32}$$

Equations (29) and (30) describe a reduced-dimension stochastic system in which the fast direction associated to the eigenvalue λ_1 has been eliminated.

3. Application: seasonally forced epidemics

3.1. Model definition and deterministic treatment

The SEIR model is a simplified epidemiological model describing the spread of a disease through a population [**?**]. Members of the population may be in one of four states: susceptible (S), exposed (E), infectious (I) and recovered (R). The susceptible individuals come into contact with the infected and become infected themselves with infection rate $\beta(t)$, may vary with time. Those exposed to the disease then become infectious with a rate of disease onset α. Finally, the infectious recover with an average rate of γ. In addition to these disease dynamics, there is a constant birth and death rate μ; it is traditional to hold the population size constant by treating death and birth as a single process whereby an individual returns to the susceptible state. As in the earlier ecological model of section 2.2, the dynamics may be conveniently summarised using the notation of chemical reactions:

Infection:	$S \xrightarrow{\beta} E$	Incubation:	$E \xrightarrow{\alpha} I$
Recovery:	$I \xrightarrow{\gamma} R$	Death/Birth:	$E, I, R \xrightarrow{\mu} S\,.$

We write $n_S\,, n_E\,, n_I\,, n_R$ for the number of individuals in states S, E, I and R, respectively. The total population size is then given by $N = n_S + n_E + n_I + n_R$, which does not vary, meaning that there are three degrees of freedom. With just a slight abuse of notation we introduce variables $S = n_S/N$, $E = n_E/N$ and $I = n_I/N$ which describe the population density of individual in each disease state. Note that there is no need for a variable associated to the recovered state, since the conservation of total population makes it a dependant variable. In the limit of large population size, an effective SDE description of the model may again be derived using the expansion detailed in [**?**]. We obtain

$$\begin{aligned}
\frac{dS}{dt} &= \mu(1-S) - \beta(t)SI + \eta_1(t)\,,\\
\frac{dE}{dt} &= \beta(t)SI - (\mu+\alpha)E + \eta_2(t)\,,\\
\frac{dI}{dt} &= \alpha E - (\mu+\gamma)I + \eta_3(t)\,,
\end{aligned} \tag{33}$$

where $\eta_{1,2,3}$ are Gaussian white noise variables with correlations

$$\Big\langle \eta_i(t)\eta_j(t')\Big\rangle = \frac{1}{N}\,\delta(t-t')B_{ij}\,,$$

$$B = \begin{pmatrix} \mu(1-S)+\beta(t)SI & -\mu E+\beta(t)SI & -\mu I \\ -\mu E+\beta(t)SI & \beta(t)SI+(\mu+\alpha)E & -\alpha E \\ -\mu I & -\alpha E & \alpha E+(\mu+\gamma)I \end{pmatrix} . \quad (34)$$

We begin by discussing the behaviour of the model in the deterministic limit $N \to \infty$. When the infection rate is not seasonally forced, so $\beta(t) \equiv \beta$, there are a pair of fixed points. The first of these represents the extinction of the disease: $S = 1\,, E = 0\,, I = 0$. The second fixed point has coordinates

$$S^* = \frac{(\alpha+\mu)(\gamma+\mu)}{\alpha\beta}\,, \quad E^* = \frac{\mu(1-S_*)}{\alpha+\mu}\,, \quad I^* = \frac{\alpha\mu(1-S_*)}{(\alpha+\mu)(\gamma+\mu)}\,, \quad (35)$$

and is referred to as the endemic state. We are concerned with the regime in which the endemic state is stable and the extinct state is unstable, which holds for a range of epidemiologically realistic parameter values. To order one in the small parameter μ, the eigenvalues of the Jacobian at the endemic state are

$$\lambda_1 = -(\alpha+\gamma) - \mu\,\frac{\alpha(2\alpha+\beta)+3\alpha\gamma+2\gamma^2}{(\alpha+\gamma)^2}\,, \quad (36)$$

and the complex-conjugate pair

$$\lambda_{2,3} = \mu\,\frac{\alpha^2\beta+\beta\gamma^2+\alpha\gamma(\beta+\gamma)}{2\gamma(\alpha+\gamma)^2} \pm -i\sqrt{\mu\,\frac{\alpha(\beta-\gamma)}{\alpha+\gamma}}\,. \quad (37)$$

Notice that we have a separation of time-scales: $\mathrm{Re}[\lambda_1] \ll \mathrm{Re}[\lambda_{2,3}]$, meaning that λ_1 corresponds to a highly stable direction. This behaviour has been previously noted and exploited in the deterministic setting [**?**]. In addition, the imaginary parts of $\lambda_{2,3}$ are an order larger than the real parts, meaning that we may expect highly oscillatory trajectories in the neighbourhood of the endemic state. We can thus expect the system to first collapse rapidly in the direction of the first eigenvector, followed by a slow, almost-planar, spiralling decay to the endemic state.

Introducing a seasonal forcing of the infection rate creates an additional layer of complexity. A typical choice would be

$$\beta(t) = \beta_0\Big(1+\delta\cos(2\pi t)\Big)\,, \quad (38)$$

where β_0 describes the basal infection rate, δ is the forcing amplitude, and time is measured in years. The deterministic system will now not settle to the endemic state, but instead exhibit limit cycle behaviour. For the sake of simplicity, we will consider only parameter values which result in a single stable limit cycle of period $T = 1$.

Similar to linear stability analysis of fixed points, there is a well-developed theory for analysing perturbations around limit cycles. We begin by writing $(S^*(t), E^*(t), I^*(t))$ for the limit cycle and introducing the vector

$$\boldsymbol{x}(t) = \begin{pmatrix} S(t)-S^*(t) \\ E(t)-E^*(t) \\ I(t)-I^*(t) \end{pmatrix} . \quad (39)$$

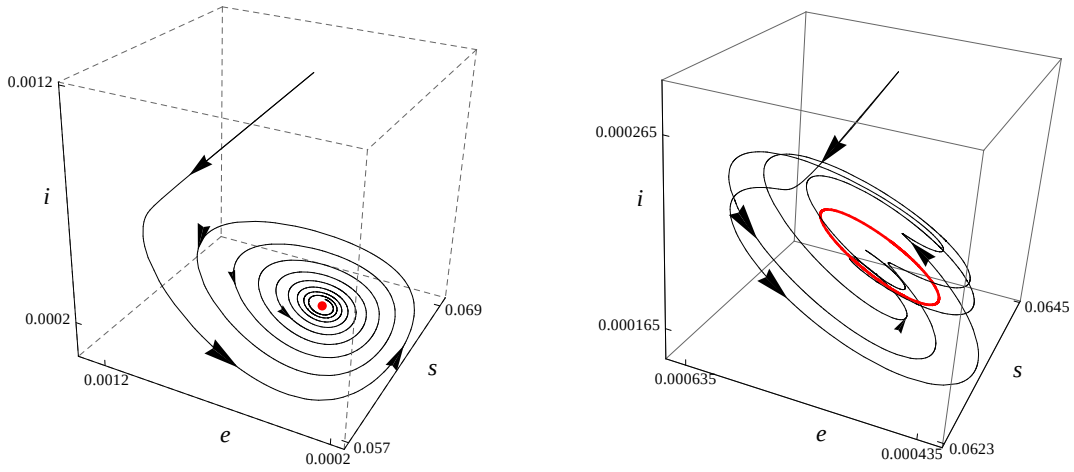

Figure 3. Deterministic trajectories for the SEIR model. Left: No seasonal forcing ($\delta = 0$), fixed point shown in red. Right: system in the presence of forcing, ($\delta = 0.02$), limit cycle highlighted in red. Remaining parameters in both plots are $\beta_0 = 1575$, $\alpha = 35.84$, $\gamma = 100$ and $\mu = 0.02$

To first order, the dynamics of $\boldsymbol{x}$ are governed by

$$\frac{d\boldsymbol{x}}{dt} = J(t)\boldsymbol{x}\,, \tag{40}$$

where J is the time-dependant Jacobian of (33). This equation may be solved using Floquet theory [6]. The key result of the theory states that solution trajectories may be decomposed into the product of a periodic vector with an exponentially growing/decaying amplitude. General solutions are of the form

$$\boldsymbol{x}(t) = \sum_{i=1}^{n} c_i \boldsymbol{p}_i(t) e^{\sigma_i t}\,, \tag{41}$$

where is the number of degrees of freedom in the model, c_i is a constant, $\boldsymbol{p}_i(t)$ a periodic vector with the same period T as the limit cycle, and the value σ_i determining the rate of growth/decay is referred to as the Floquet exponent. Akin to eigenvalues, Floquet exponents are indicative of the stability of the limit cycle in the time-varying directions $\boldsymbol{p}_i(t)$; perturbations to the trajectory will grow if $\mathrm{Re}[\sigma_i] > 0$ and decay if $\mathrm{Re}[\sigma_i] < 0$.

In all but the most trivial examples, obtaining the Floquet exponents and periodic vectors must be carried out numerically. The procedure (detailed in appendix B) requires first computing a matrix whose columns are independent trajectories, $X(t) = (\boldsymbol{x}_1(t) \cdots \boldsymbol{x}_n(t))$, and then *accurately* inverting $X(T)$. However, if there is a rapid collapse along a stable direction, then the columns of $X(T)$ will be almost linearly dependant, since all solution trajectories quickly move towards the same plane. This will make the determination of the inverse of $X(T)$ prone to large numerical errors which will spoil the rest of the procedure. This problem was previously highlighted in [**?**], prompting the authors to implement arbitrary precision numerical methods, at a considerable cost of computing time.

3.2. Stochastic treatment exploiting the slow manifold

Beginning with the unforced case, we let λ_1, λ_2 and λ_3 be as in (36, 37) and write $\boldsymbol{v}_1$, $\boldsymbol{v}_2$, $\boldsymbol{v}_3$ for the corresponding eigenvectors. Introduce the transformation matrix $V = (\boldsymbol{v}_1 \quad (\boldsymbol{v}_2 + \boldsymbol{v}_3) \quad i(\boldsymbol{v}_2 - \boldsymbol{v}_3))^T$ and new variables

$$\begin{pmatrix} y \\ z_1 \\ z_2 \end{pmatrix} = V \begin{pmatrix} S \\ E \\ I \end{pmatrix} . \tag{42}$$

The Jacobian of the transformed system at the endemic fixed point takes the form

$$J' = \begin{pmatrix} \lambda_1 & 0 \\ 0 & L \end{pmatrix} + \mathcal{O}(\mu^{3/2}) , \quad \text{where} \quad L = \begin{pmatrix} \mathrm{Re}[\lambda_2] & \mathrm{Im}[\lambda_3] \\ \mathrm{Im}[\lambda_2] & \mathrm{Re}[\lambda_3] \end{pmatrix} . \tag{43}$$

The nullcline for y is determined by manipulating equation (27) into the form $y = \theta(z_1, z_2)$, with $\boldsymbol{A}$ copied from equation (33). Although an explicit form for θ can be found, the expression is far too complicated to be worth reproducing here.

To capture the effects of stochasticity, we introduce variables describing the error in the new coordinates, rescaled by a factor of $\sqrt{N}$,

$$\boldsymbol{\xi} = \sqrt{N} \begin{pmatrix} y - y^* \\ \boldsymbol{z} - \boldsymbol{z}^* \end{pmatrix} . \tag{44}$$

Making this substitution in (33) and keeping only first order terms in N and μ, we find that $\boldsymbol{\xi}$ obeys

$$\frac{d\boldsymbol{\xi}}{dt} = J'\boldsymbol{\xi} + \boldsymbol{\zeta}(t) , \tag{45}$$

where

$$\langle \zeta_i(t)\zeta_j(t') \rangle = \delta(t - t')B'_{ij} . \tag{46}$$

The matrix B' is given by

$$B' = VBV^T \Big|_{(S,E,I)=(S^*,E^*,I^*)} , \tag{47}$$

where B is as in (34). Note that applying the constraint $y = \theta(z_1, z_2)$ induces the relationship

$$y^* + \frac{\xi_1}{\sqrt{N}} = \theta\left(z_2 + \frac{\xi_2}{\sqrt{N}}, z_3 + \frac{\xi_3}{\sqrt{N}} \right) . \tag{48}$$

Expanding once more in large N, we find

$$\xi_1 = \left[\xi_2 \frac{\partial\theta}{\partial z_2} + \xi_3 \frac{\partial\theta}{\partial z_3} \right|_{\boldsymbol{z}=\boldsymbol{z}^*} . \tag{49}$$

After elimination of the fast direction, equation (44) becomes

$$\frac{d}{dt} \begin{pmatrix} \xi_2 \\ \xi_3 \end{pmatrix} = L \begin{pmatrix} \xi_2 \\ \xi_3 \end{pmatrix} + \begin{pmatrix} \zeta_2(t) \\ \zeta_3(t) \end{pmatrix} , \tag{50}$$

where ζ_2 and ζ_3 have correlation matrix B'', which is related to B' by equation (32).

We move on now to study the situation of seasonally forced infection rate. In principle, the calculations above apply only in the limit of small forcing amplitude (that is, $\delta \to 0$ in (38)). We learnt in the ecological example, however, that although our theory is developed to apply in the locality of a stable fixed point, it can continue to provide a useful approximation if this condition is violated. Applying that lesson to the present case, we take the foolhardy step of modifying equation (50) to allow L and B'' to become functions of time, as dictated by the replacement $\beta \mapsto \beta(t)$. Essentially, we are approximating the limit cycle by its projection to the nullcline of the fast direction at the endemic fixed point of the unforced model, and then forcing any stochastic fluctuations to remain on this nullcline.

A Floquet analysis of the deterministic part of the reduced system finds two complex conjugate Floquet multipliers, with the third disparate multiplier having been eliminated from the system. This system no longer suffers from the numerical difficulties which plague the full three-dimensional model.

To quantify the effect of stochastic fluctuations in this model, we follow the standard procedure of computing the autocorrelation matrix $C(\tau)$ of oscillations around the limit cycle, which has entries

$$\Big[C(\tau)\Big]_{ij} = \frac{1}{N}\int_0^T \Big\langle \xi_i(t)\xi_j(t+\tau)\Big\rangle dt\,. \tag{51}$$

Of course our reduced system (50) is two-dimensional, meaning that the entries of C pertaining to ξ_1 must be deduced from equation (49). The coordinate transformation applied at the start in (42) may then be inverted to give the autocorrelation matrix for errors in S, E and I.

The Fourier transform of the diagonal entries of the autocorrelation gives the power-spectrum of oscillations, which provides a convenient visualisation of any stochastic oscillations. In Figure 4 we plot the power-spectrum of oscillations around the limit cycle affecting the number of infected individuals, comparing between stochastic simulations and the theoretical prediction using the reduced-dimension model (50). The peaks in the approximate theoretical spectra are found at the same positions as those for the simulated spectra. These are given by

$$v_j = \frac{j}{T} \pm \frac{|\mathrm{Im}[\rho_{1,2}]|}{2\pi}\,. \tag{52}$$

The overall benefit that was garnered by the procedure however was that of time. The computation of the theoretical power spectra approximated from the reduced system takes takes a fraction of the computing time/power of the full system.

4. Conclusions

Appendix A.

In this appendix a brief review is given of the methods which lead from a microscopic interaction model to a stochastic differential equation of the type used in this paper

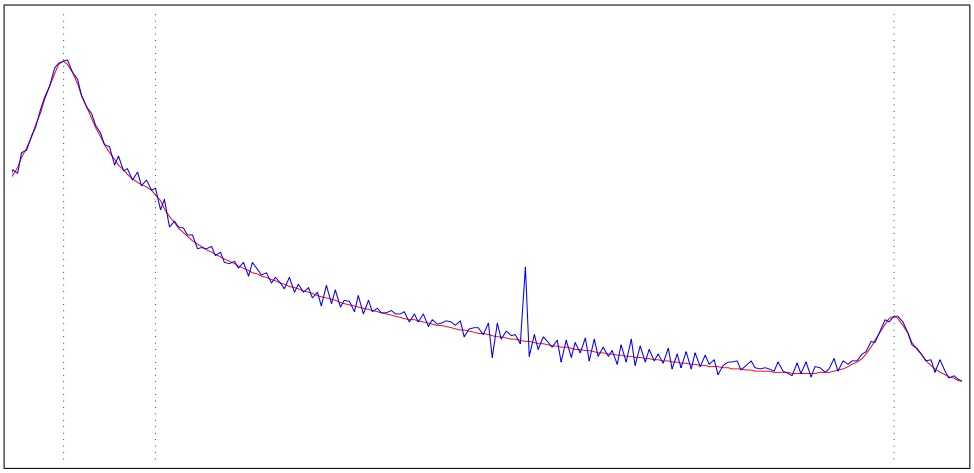

Figure 4. Power spectra for the fluctuations in the number of infected about the limit cycle. Parameters go here.

(Eqns **??**)

Consider a system described by discrete state variables, $\mathbf{n}$, where $\mathbf{n}$ is a vector of integers. Rather than describing the dynamics in terms of the time evolution of the state of the system, the dynamics may instead be described by the time evolution of the probability distribution of the state of the system. This description is given by the master equation [**?**]; the rate of change of the probability of occupancy of a state $\mathbf{n}$, $p(\mathbf{n})$ given a transition rates between states $T(\mathbf{n}|\mathbf{n}')$ is

$$\frac{\partial p(\mathbf{n},t)}{\partial t} = \sum_{n} [T(\mathbf{n}|\mathbf{n}')(t)p(\mathbf{n}',t) - T(\mathbf{n}'|\mathbf{n})(t)p(\mathbf{n},t)]. \tag{A.1}$$

While the master equation describes the dynamics of the system entirely, it is not analytically tractable. A particular realisation of a process obeying the master equation may be exactly simulated using the Gillespie algorithm [**?**]. While the simulation does not necessarily provide as deep an understanding of the behaviour of the system, it provides a useful comparison for analytical techniques.

To make analytical progress, the diffusion limit is taken. Rather than considering the discrete state variables $\mathbf{n}$, state variables $\mathbf{x}$ are introduced as a measure of the discrete state variables scaled by some measure of the system size ϵ, such that $\mathbf{x} = \epsilon\mathbf{n}$. The vector $\mathbf{x}$ can then be said to be approximately continuous in the limit of small ϵ. One may then truncate the Kramers-Moyal expansion of the master equation (an exact Taylor expansion in terms of jump-moments) at second order in ϵ to arrive at a Fokker-Planck equation [12] describing the evolution of the probability density function;

$$\frac{\partial p(\mathbf{x},t)}{\partial t} = -\sum_{i=1}^{2} \frac{\partial}{\partial x_i}(A_i(\mathbf{x})p(\mathbf{x},t)) + \frac{\epsilon}{2}\sum_{i,j=1}^{2} \frac{\partial^2}{\partial x_i \partial x_j}(B_{ij}(\mathbf{x})p(\mathbf{x},t)). \tag{A.2}$$

The vector $\mathbf{A}(\mathbf{x})$ and the matrix $B(\mathbf{x})$ can be expressed explicitly in terms of the probability transition rates. This Fokker-Planck equation can be shown to be entirely

equivalent to a stochastic differential equation, or SDE, of the form

$$\frac{d\mathbf{x}}{dt} = \mathbf{A}(\mathbf{x}) + \epsilon\boldsymbol{\eta}(t) \tag{A.3}$$

where an Itō formulation of stochastic calculus has been employed [11]. Here $\boldsymbol{\eta}(t)$ is as usual a Gaussian white noise term such that $\langle \underline{\eta}(t)\rangle = 0$ and $\langle \eta_i(t)\eta_j(t')\rangle = B_{ij}\delta(t-t')$. For systems of some fixed size N, it can make intuitive sense to set ϵ as an explicit measure of the system size; $\epsilon = 1/N$.

For the illustrative example in section 2.2 the transition rates for the discrete vector (X, Y) can be taken from the reaction equations decribing the system. For instance

$$T(X+1, Y|X, Y) = (1-\mu)X + \epsilon(\frac{1}{2} - p)X^2 \tag{A.4}$$

$$T(X, Y-1|X, Y) = \epsilon(\frac{1}{2} + p)XY + \epsilon(\frac{1}{2} - p)YY. \tag{A.5}$$

Tthe discrete variables X and Y have been scaled by the system size measure ϵ to arrive at a stochastic differential equation in the approximately continuous variables $x = \epsilon X$ and $y = \epsilon Y$ using the methods outlined above.

The same methods have been used to move from a microscopic epidemic model described in section 3 to the macroscopic stochastic differential equation presented.

Appendix B.

The analogue of a linear stability analysis for systems with periodic components is known as Floquet theory [6]. It can also play an important role in the analysis of stochastic fluctuations about a deterministic trajectory [1] [13]. In this appendix the general formulation of Floquet theory is discussed before the more detailed application to linear stochastic systems is given.

Floquet theory gives the solutions to sets of linear differential equations in the form of Equation (**??**), where $J(t)$ is periodic with a period T. The general solution can be shown to be

$$\boldsymbol{x}(t) = \sum_{i=1}^{n} c_i \boldsymbol{p}_i(t) e^{\sigma_i t}, \tag{B.1}$$

where $\boldsymbol{p}(t)$ is a periodic vector and σ_i are termed the Floquet exponents of the system. The quantities $\rho_i = e^{\sigma_i T}$ are termed the Floquet multipliers of the system.

In particular one can work in a canonical form for calculational ease, with canonical quantities denoted with a subscript 0. The canonical form is constructed from n decomposed solutions to equation Equation (**??**) such that $x(t)_i = \boldsymbol{p}_i(t)e^{\sigma_i t}$. A fundamental matrix of these solutions may then be introduced along with matrices Y_0 and P_0;

$$X_0 = [\boldsymbol{\xi}_0^1(t), \boldsymbol{\xi}_0^2(t), \boldsymbol{\xi}_0^3(t)], \tag{B.2}$$

$$X_0 = P_0 Y_0, \tag{B.3}$$

$$P_0 = [\boldsymbol{p}_0^1(t), \boldsymbol{p}_0^2(t), \boldsymbol{p}_0^3(t)], \tag{B.4}$$

$$Y_0 = Diag[e^{\mu_i t}]. \tag{B.5}$$

A method for obtaining the Floquet multipliers μ_i along with the canonical form of the solutions is now required. Obtaining both is dependent on the determination of the monodromy matrix.

The monodromy matrix, D, is defined such that $X(t+T) = X(t)D$, for any fundamental matrix $X(t)$ constructed from linearly independent solutions to REF. It can be shown that while the monodromy matrix is dependent on the fundamental matrix chosen [6], its eigenvalues are independent and are a property of the system. The eigenvalues of D are ρ_i, the Floquet multipliers of the system. Further, if a matrix W is constructed from the eigenvectors of D, the canonical fundamental matrix $X_0(t)$ may be shown to be related to a general fundamental matrix $X(t)$ via $X_0(t) = X(t)W$. Therefore, the monodromy matrix allows the canonical fundamental matrix $X_0(t)$ to be determined from a general fundamental matrix $X(t)$, along with the matrix $\mathbf{Y}_0$. From these the periodic matrix $P_0(t)$ may then also be deduced.

If the system under consideration displays limit cycle behaviour, the preceding analysis must evidently be carried out numerically. In general a fundamental matrix obtained numerically will have to be transformed into canonical form by a numerical determination of the mondromy matrix, $D = X^{-1}(t)X(t+T)$.

Now the stochastic system may be considered;

$$\frac{d\boldsymbol{\xi}}{dt} = J(t)\boldsymbol{\xi} + \boldsymbol{\eta}(t)\,, \tag{B.6}$$

The solution may be constructed as a sum of the general solution to Equation (**??**) along with a particular solution, so that

$$\boldsymbol{\xi}(t) = X_0(t)\boldsymbol{\xi}_0 + X_0(t)\int_{t_0}^{t} X_0^{-1}(s)\boldsymbol{\eta}(s)ds, \tag{B.7}$$

or, setting the initial conditions in the infinite past and making a change of integration variable $s \to s' = t - s$

$$\boldsymbol{\xi}(t) = P_0(t)\int_{t_0}^{t} Y(s')P_0^{-1}(t-s')\boldsymbol{\eta}(t-s')ds'. \tag{B.8}$$

In the course of the analysis conducted in section 3, $\xi(t)$ represents some stochastic fluctuation around limit cycle behaviour. An obvious quantity of relevance is the power spectrum of such fluctuations. To obtain the power spectrum, one may first obtain the two time correlation function $C(t+\tau, t) = \langle \boldsymbol{\xi}(t+\tau)\boldsymbol{\xi}^T(t)\rangle$, from this obtain the autocorrelation function, and then employ the Weiner-Khinchin theorem.

$$P_i(\omega) = \int C_{ii}(\tau)e^{i\omega\tau}d\tau, \tag{B.9}$$

$$C_{ij}(\tau) = \frac{1}{\tau}\int_{0}^{T} P_0(t+\tau)Y_0(\tau)\Lambda(t)P_0^T(t)dt \tag{B.10}$$

$$\Lambda(t) = \int_{t_0}^{\infty} Y(s)\Gamma(t-s)Y(s)ds \tag{B.11}$$

$$\Gamma(s) = P_0^{-1}(s)\Psi(s)P_0^{-1}(s)]^T. \tag{B.12}$$

The intermediate steps are left to the reader, but full details are found in [2]. A key point to note is that these results hold *only* for the canonical matrices X_0, P_0 and Y_0.

[1] A.J. Black, A.J. McKane. Stochastic amplification in an epidemic model with seasonal forcing. *J. Theor. Biol.*, 267:85–94, 2010.

[2] R.P. Boland, G. Galla, and A.J. McKane. Limit cycles, floquet multipliers, and intrinsic noise. *Phys. Rev. E*, 79:051131, 2009.

[3] C.W. Gardiner. Adiabatic elimination in stochastic systems. i. formulation of methods and appliction to few-variable systems. *Phys. Rev. A*, 29, 1984.

[4] C.W. Gardiner. *Handbook of Stochastic Methods*. Springer, Berlin, 2009.

[5] D. T. Gillespie. A general method for numerically simulating the stochastic time evolution of coupled chemical reactions. *J. Comp. Phys.*, 22:403–434, 1976.

[6] R. Grimshaw. *Nonlinear Ordinary Differential Equations*. CRC Press, Oxford, 1990.

[7] H. Haken and G. Schöner. The Slaving Principle for Stratanovich Stochastic Differential Equations. *Z. Phys. B.*, 63:493–504, 1986.

[8] H. Haken and G. Schöner. A Systematic Elimination Procedure for Itō Stochastic Differential Equations and the Adiabatic Approximation. *Z. Phys. B.*, 68:89–103, 1987.

[9] H. Haken and A. Wunderlin. Generalized Ginzburg-Landau Equations, Slaving Principle and Center Manifold Theorem. *Z. Phys. B.*, 44:135–141, 1981.

[10] H. Haken and A. Wunderlin. Slaving Principle for Stochastic Differential Equations with Additive and Multiplicative Noise and for Discrete Noisy Maps. *Z. Phys. B.*, 47:179–187, 1982.

[11] K. Jacobs. *Stochastic Processes for Physicists*. Cambridge University Press, Cambridge, 2010.

[12] H. Risken. *The Fokker-Planck Equation*. Springer, Berlin, 1989.

[13] G. Rozhnova and A. Nunes. Stochastic effects in a seasonally forced epidemic model. *Phys. Rev. E*, 82:041906, 2010.

[14] I. B. Schwartz and H. L. Smith. Infinite subharmonic bifurcation in an seir epidemic model. *J. Math. Biol.*, 18:233–253, 1983.

[15] R. Serra, M. Andretta, M Compiani, and G Zanarini. *Introduction to the Physics of Complex Systems*. Pergamon Press, Oxford, 1986.

[16] N. G. van Kampen. *Stochastic Processes in Physics and Chemistry*. Elsevier, Amsterdam, 2007.